International Journal of Technology 10(1): 147-158
ISSN 2086-9614

MORPHOLOGICAL AND STRUCTURAL STUDY OF VERTICALLY ALIGNED ZINC OXIDE NANORODS GROWN ON SPIN COATED SEED LAYERS

Albertus Bramantyo[1,2*], Kenji Murakami[1], Masayuki Okuya[1], Arief Udhiarto[2], Nji Raden Poespawati[2]

[1]*Faculty of Engineering, Shizuoka University, 3-5-1 Johoku, Naka-ku, Hamamatsu, 432-8561, Japan*
[2]*Department of Electrical Engineering, Faculty of Engineering. Universitas Indonesia, Kampus UI Depok, Depok 16424, Indonesia*

(Received: May 2018 / Revised: June 2018 / Accepted: October 2018)

ABSTRACT

In this study, vertically aligned zinc oxide (ZnO) nanorod (NR) arrays were grown with the 2-step method. Spin coating was used to apply the seed layer, and by increasing the number of repetitions (*n*), higher thickness of the seed layer was achieved. The effects of different seed layer thicknesses, spin coated at different rotational speeds (*v*) and how the variables (*v* and *n*) influence the morphological and crystal properties of the resulting ZnO NRs were analyzed. The effects of 1, 3, and 5 (*n*), with (*v*) of 3000 or 4000 rpm were investigated, and the formed seed layers were characterized by using scanning electron microscopy (SEM) and X-ray diffraction (XRD) profiles. The ZnO NR arrays were grown by a chemical bath deposition method because of its simplicity and ease of use. Full width at half maximum (FWHM) analysis was conducted on the XRD chart and Raman spectrum to analyze the grain size and Wurtzite distortion of the ZnO NRs. A lower FWHM value was attributed to the lower number of structural disorders in the ZnO NRs, which equated to the most stable or structured Wurtzite structures in the ZnO NRs, achieved at the lowest FWHM value. The lowest FWHM for (002) XRD peak was obtained at 0.35° for ZnO NRs grown with a seed layer spin coated at 4000 rpm once. The crystallite size calculated by Scherrer's equation gave a size of 25.14 nm. The lowest FWHM for E_2(High) Raman peak was obtained at 6.00 cm^{-1} for ZnO NRs grown with a seed layer spin coated at 4000 rpm three times.

Keywords: Chemical bath deposition; Nanorods; Spin coating; Vertical growth; ZnO

1. INTRODUCTION

Numerous studies of zinc oxide (ZnO) materials have been conducted because of the semiconductor properties with direct bandgap energy of 3.37 eV and high exciton binding energy of 60 meV at room temperature. One motive for such studies is that one-dimensional (1-D) ZnO materials have excellent optical properties, having varying shapes such as nanorods/nanowires, nanobelts or nanoflowers. They can be applied as chemical sensors, photodetectors, field-effect transistors (FET) or solar cells, amongst other uses. ZnO material is environmental friendly and does not have a harmful effect on the environment. Due to their biocompatibility, ZnO materials can be applied to biochemical, medical, or other related fields. A study conducted by (Kashif et al., 2012) was conducted to compare ZnO nanorods (NRs) made by KOH-based and monoethanolamine-based seed layers (Kashif et al., 2012).

*Corresponding author's email: bramantyoalbertus@gmail.com, Tel. +62-815-9105417
Permalink/DOI: https://doi.org/10.14716/ijtech.v10i1.2012

ZnO NRs with higher electrical conductivity are better suited to power-saving optoelectrical devices, while those with better crystallinity alignment have properties such as higher longevity and stability and are suitable for optoelectronic applications. Vertically aligned ZnO NRs with a hexagonal Wurtzite structure have high piezoelectric and pyroelectric properties. They can also be used to grow nanotubes or core-shell nanowires. One of the methods to grow 1-D ZnO nanostructures is the vapor-liquid-solid (VLS) method, in which a substrate with seed droplets is exposed to vapor particles in a chamber to form solid nanowires. Another method to grow 1-D ZnO nanostructures is chemical vapor deposition (CVD), which involves the use of a gas chamber and application by thermal treatment.

Several papers have mentioned the importance of seed layers in growing vertically aligned ZnO NRs. By controlling the thickness of the seed layer, the resulting nanorod size, alignment and density can be manipulated (Peiris et al., 2013). Higher seed layer thickness yields increased grain and particle size (Ghayour et al., 2011). In the case of a very thick seed layer, its density decreases along with the nucleation sites (İkizler & Peker, 2014). One method to control the grain size of the seed layer is to control the temperature of the annealing treatment employed (Wahid et al., 2013; Yoon et al., 2015; Gautam et al., 2016). Thermal treatment of the seed layer also affects the (002) crystallinity after the seed has grown into nanorods. A combination of seed layer thickness and thermal treatment makes ZnO NRs suitable for photovoltaic applications (Sholehah & Yuwono, 2015). The vacancy of oxygen atoms or molecules on the seed surface increases with the temperature. (Dou et al., 2015) researched another method of controlling ZnO NR morphology by adding Ga dopants to the ZnO seed layer (Dou et al., 2015). The addition of a dopant affects the density of the seed layer, and by changing its concentration, the resulting diameter or length of the NRs can also be controlled. A similar method can be applied with the addition of polyethyleneimine (PEI) chemical to the seed layer solution and/or NR growth solution (Huang et al., 2011; Poornajar et al., 2016). Another method to control the seed layer is to change the concentration of the seed layer solution (Pourshaban et al., 2015) or to increase the length of the growth process (Kurda et al., 2015). With a higher annealing temperature, the crystallinity in the (002) direction experiences higher intensity, which leads to vertically alignment and longer NR length (Kim et al., 2014a). Post-hydrothermal treatment of the ZnO NRs also affects their crystallinity (Sholehah et al., 2017).

Many studies have been conducted on vertically aligned ZnO NRs because of their improved photovoltaic properties. This paper aims to provide an alternative way of studying the effects of various thicknesses of the seed layer by spin coating performed with differing numbers of cycles (*n*). The spin coating method was chosen due to its simplicity and ability to control the thickness of the deposited seed layer by adjusting the rotational speed (*v*). Characterizations by X-ray diffraction (XRD) and Raman spectroscopy were conducted to provide morphological analysis. Full width at half maximum (FWHM) analysis was performed on the two characterizations to provide more depth to the morphological analysis. The analyses reveal that the FWHM value is linked to the variable *n* in the form of charts.

The research conducted by Song and Lim concluded that by adding dopant atoms to the seed layers and by manipulation of seed layer thickness, the morphology and crystallinity of the ZnO NRs were also affected (Song & Lim, 2007). Several studies have combined the techniques of zinc seed layers containing dopant atoms with TiO_2 materials to increase the photovoltaic parameters (Kim et al., 2014b). In this paper, a method to control the morphology and density of the seed layer is proposed by changing the number of cycles (*n*) of the spin coating at different rotational speeds (*v*) of 3000 and 4000 rpm. By controlling the number of *n*, control of the surface of the seed layer and the sizes of the resulting ZnO NRs, together with their crystallinity, is possible.

2. METHODS

The experimental method of this paper was inspired by former work on ZnO NRs by a colleague (Winantyo et al., 2017). Normal glass substrates were cleaned ultrasonically for 5 minutes with distilled water, acetone and ethanol separately. 0.7 g of zinc acetate dihydrate was mixed with 20 mL of 2-methoxyethanol solution in order to prepare the seed layer solution. Ten drops of ethanolamine were added to the solution to act as a stabilizer. The solution was then stirred and heated at 60°C for 20 min before being spin coated homogenously onto the normal glass. The spin coating process was performed for 1 min at speeds (*v*) of 3000 and 4000 rpm, for comparison purposes. Next, the substrates attached to the seed layer were annealed at 100°C. For analytical purposes, the spin coating procedure followed by annealing was repeated one, three and five times before annealing at 350°C for 1 h. The following step was to grow the ZnO nanorods by the chemical bath deposition method using waterbath apparatus. The growth solution consisted of 30 mL solution of 0.03 M zinc acetate dihydrate and 30 mL solution of 0.03 M hexamethylenetetramine (HMT). The normal glass substrates coated with the seed layer were immersed into the solution. The beaker that contained the immersed samples was kept in the water, while thermal treatment was conducted at 85°C for 3 h. During the hydrothermal growth, the position of the water surface in the waterbath apparatus was monitored. If it was on the point of becoming lower than the beaker containing the samples and growth solution, the water was topped up. The growth solution did not need to be renewed until the growth process was finished. The refilling of the water was done approximately every hour after the water temperature in the waterbath machine had reached 85°C. Figure 1 shows a schematic diagram of the ZnO nanorod growth in the waterbath apparatus.

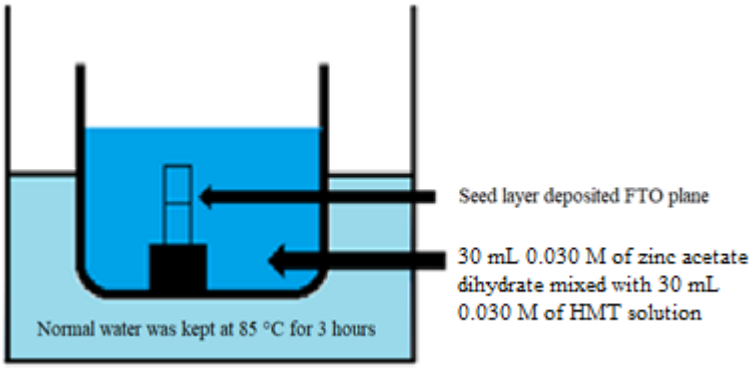

Figure 1 Growth of ZnO NRs in the waterbath machine

The formed ZnO seed layers and nanorods (NRs) were analyzed using a field-emission scanning electron microscope (FE-SEM, JEOL JSM-6320F) and X-ray diffractometer (XRD, RIGAKU Ultima III) with Cu kα radiation (λ = 1.5418 Å). A Raman Spectrum was performed with a NRS7100 Laser Raman Spectrometer. The labeling of the samples is listed in Table 1, based on the seed layer deposition parameters *v* and *n*. Scherrer's equation was used to calculate the Full Width at Half Maximum (FWHM) to the XRD and Raman peaks:

$$\tau = \frac{K\lambda}{\beta \cos\theta} \qquad \text{Scherrer's equation}$$

where τ is the crystallite size, *K* is the shape factor constant valued at 0.9 (some sources value *K* at 0.89), β is the width at FWHM (in radian value), and θ is the Bragg angle.

Table 1 Labeling of the samples based on the seed layer deposition parameters

v	*n*		
	1	3	5
3000 rpm	Seed layer: SL 31 Nanorods: NR 31	Seed layer: SL 33 Nanorods: NR 33	Seed layer: SL 35 Nanorods: NR 35
4000 rpm	Seed layer: SL 41 Nanorods: NR 41	Seed layer: SL 43 Nanorods: NR 43	Seed layer: SL 45 Nanorods: NR 45

3. RESULTS AND DISCUSSION

The seed layer provides the nucleation sites needed to grow vertically aligned ZnO nanorods. The spin coating method provided a simplistic approach; by controlling the number of repetitions, the density and geometry of the synthesized films can be controlled. The effects of the spin coating cycle (*n*) and the rotation speed (*v*) are clearly revealed on the morphology of the seed layer, as shown in Figure 3. When $n = 1$, the seed layer surface was rough. Low coverage of the seed surface contributed to the uneven spread of the seed layer. The same situation was realized for both $v = 3000$ and 4000 rpm. When the number of *n* reached 5, the surface of the seed layer became smoother and covered the entire surface of the normal glass substrate. The thickness of the seed layer also seemed to increase with the number of *n*. The results could affect the growth of ZnO NRs on the seed layer. When *v* was 4000 rpm, the resulting seed layer surface was homogenous and equally spread; however, the thickness of the seed layer was reduced compared to $v = 3000$ rpm. Observation of the thickness of the seed layer at $v = 2000$ rpm was made. With lower *v*, the thickness increased due to the lower centrifugal force applied to the center of the sample. Such a spin coating pattern also risked an uneven spread and rough surface of the seed layer. The resulting ZnO NRs became more tilted and less dense. When *n* was increased to 3 or 5 (SL33, SL35, SL43, and SL45), networks of zinc nuclei were visible. With the higher number of *n*, the density of the seed layer increased. In SL 41, a similar network could be seen, although the seed layer surface had a rough quality due to the uneven spread.

The morphologies of the ZnO NRs grown on the different seed layers were also observed by SEM, as shown in Figures 4 and 5. The diameter and thickness of the ZnO NRs is shown in Table 2. A seed layer with a rough surface or non-homogeneous distribution leads to the growth of NRs with various diameters. As the spin coating cycle for the seed layer increases, the size distribution of the NR diameters becomes narrow, with a higher NR density due to the homogeneity of the seed layer. Figure 5 shows the cross sections of the ZnO NRs grown on the different seed layers. Although the thickness of the ZnO NRs did not show a certain pattern of growth, the NRs grown at the lower speed (NR31, NR33, and NR 35) showed higher thickness due to the greater supply of zinc nuclei compared to those at the higher speed (NR41, NR43, and NR45).

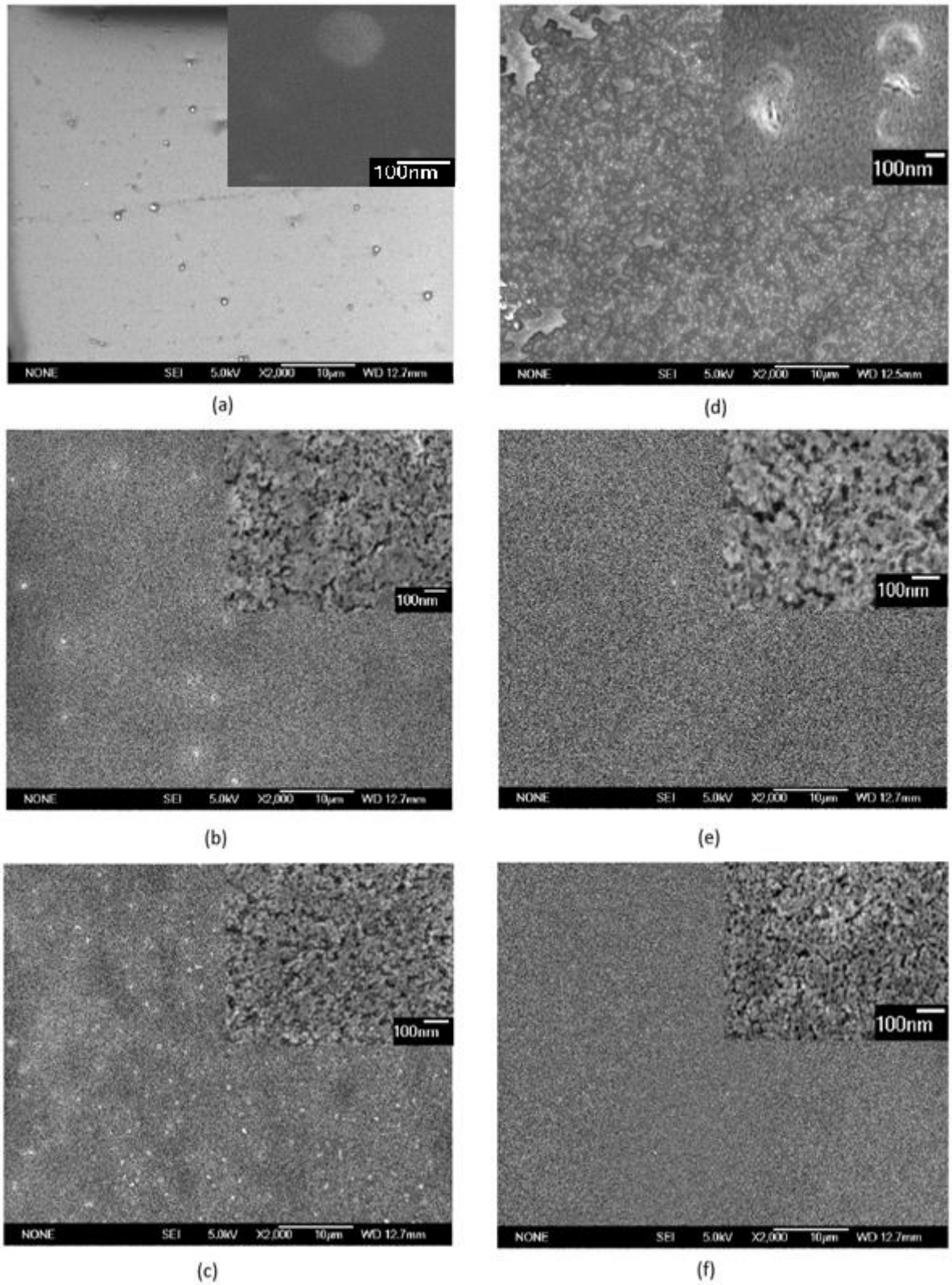

Figure 2 SEM images of the seed layers grown on normal glass for: (a) SL 31; (b) SL 33; (c) SL 35; (d) SL 41; (e) SL 43; and (f) SL 45

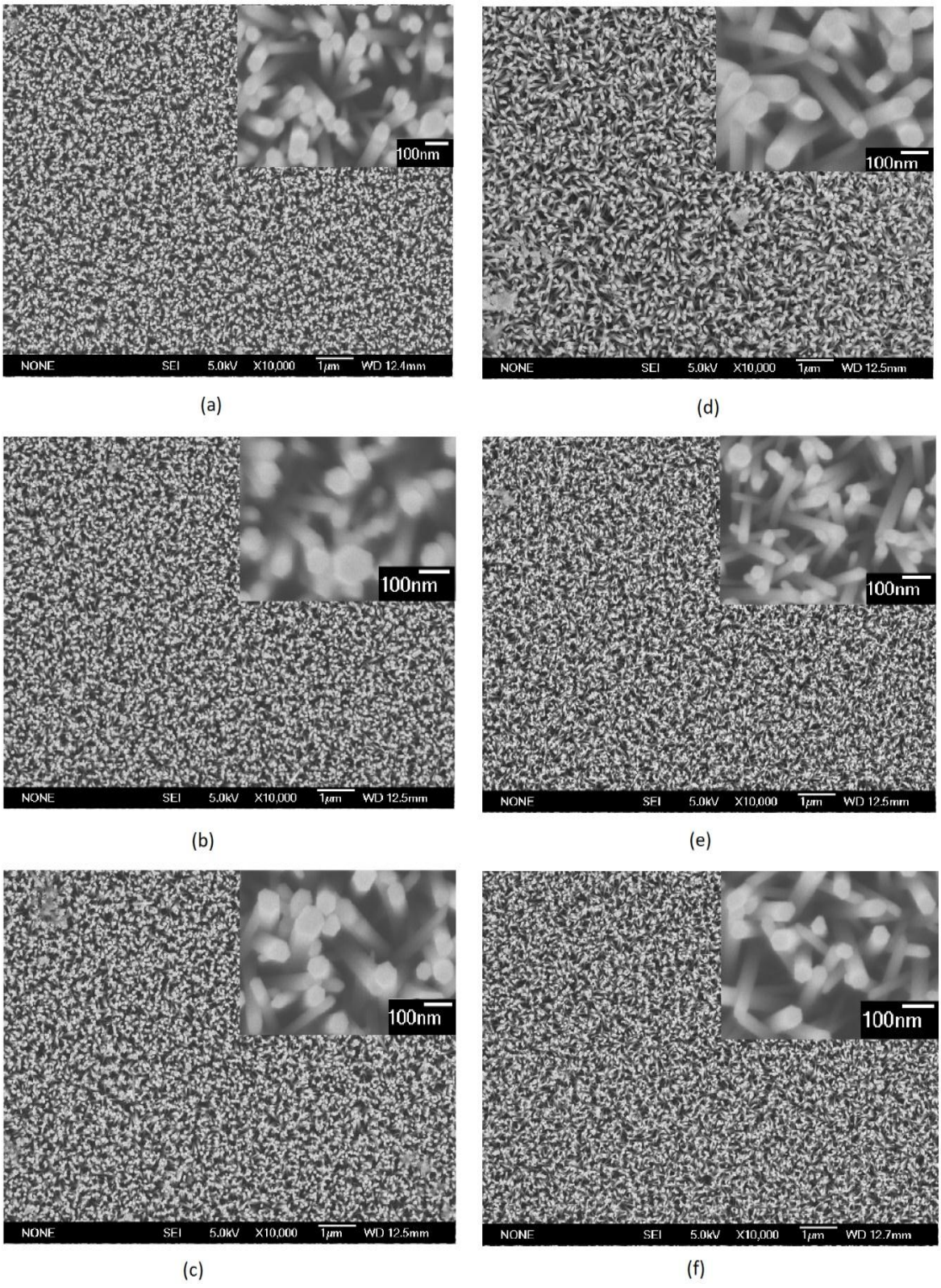

Figure 3 Top-down view of SEM images of the ZnO nanorods (NRs) on normal glass for: (a) NR 31; (b) NR 33; (c) NR 35; (d) NR 41; (e) NR 43; and (f) NR 45

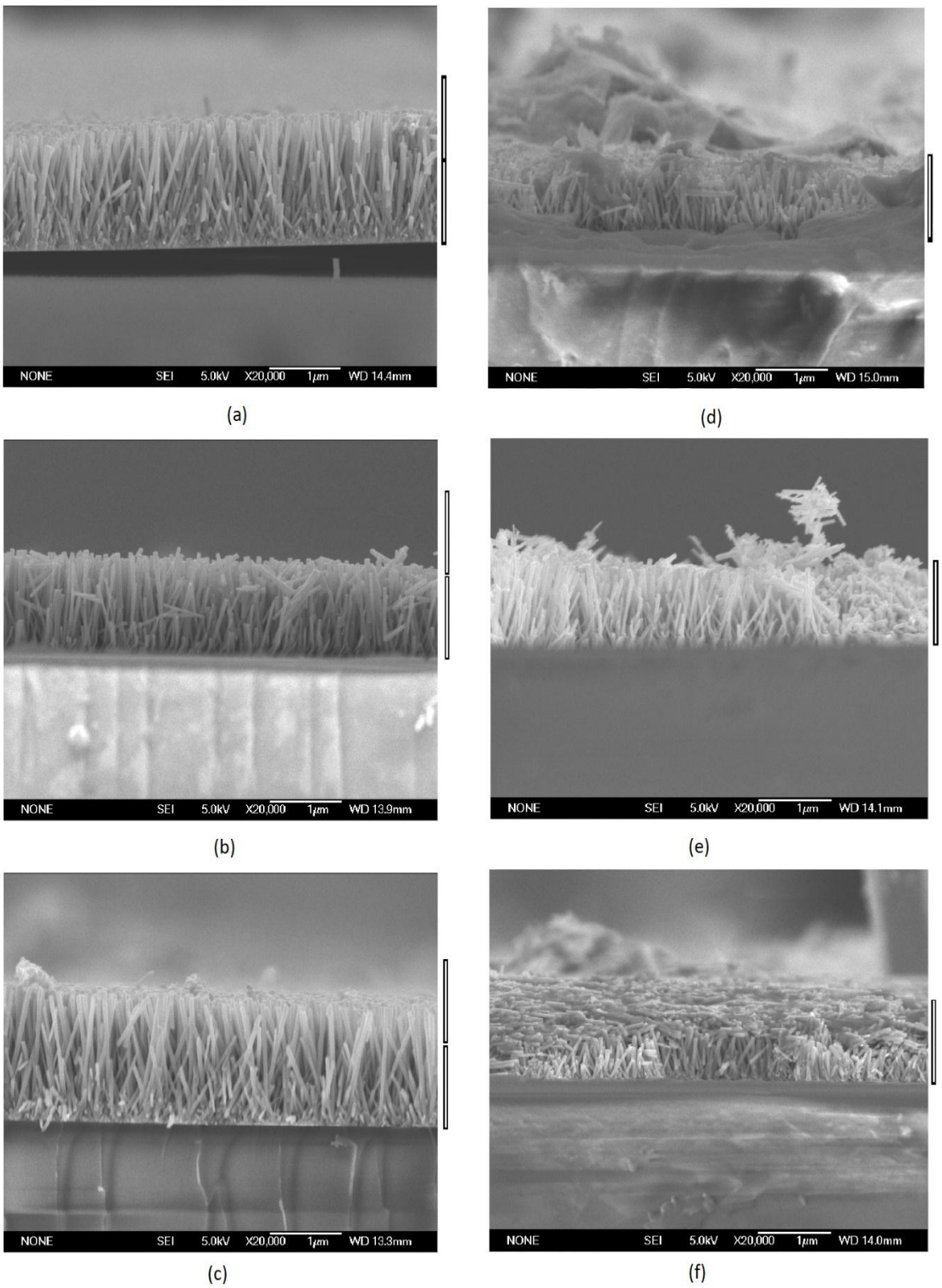

Figure 4 Cross-section view of SEM images of the ZnO nanorods (NRs) on normal glass for: (a) NR 31; (b) NR 33; (c) NR 35; (d) NR 41; (e) NR 43; and (f) NR 45

Table 2 ZnO NR diameter and thickness

v	*n*		
	1	3	5
3000 rpm	Diameter: 10–100 nm Thickness: 1.5–1.7 μm	Diameter: 10–110 nm Thickness: 1.0–1.1 μm	Diameter: 20–110 nm Thickness: 1.4–1.5 μm
4000 rpm	Diameter: 10–80 nm Thickness: 0.8–1.0 μm	Diameter: 10–70 nm Thickness: 0.8–1.0 μm	Diameter: 10–70 nm Thickness: 0.4–0.5 μm

The growth of the ZnO NRs and their corresponding XRD results show certain patterns (Figure 6). When *n* was increased (NR 33, NR35, NR43, and NR45), the crystallinity of the ZnO NRs was improved, as shown in the evolvement of (002) and (100) peaks in Figure 6, with the exception of NR41 where a considerable (100) peak is present. In the case of *v* = 4000 rpm (NR41, NR43, and NR45), notable differences were seen in the reduced size of the diameter, with the largest diameter obtained in NR41, due to the uneven spread of the seed layer, contrary to the case of *v* = 3000 rpm (NR31, NR33, and NR35). It was also found from the XRD results that higher intensities of the (002) peak confirmed the vertically aligned, c-axis oriented, growth of ZnO NRs. However, the preferred oriented growth of nanorods depended strongly on the morphology of the seed layer. A vertically aligned ZnO NR, or growth along the c-axis, delivers a reduced recombination of electrons due to the faster time needed for the generated electron to reach the FTO substrate in solar cells applications.

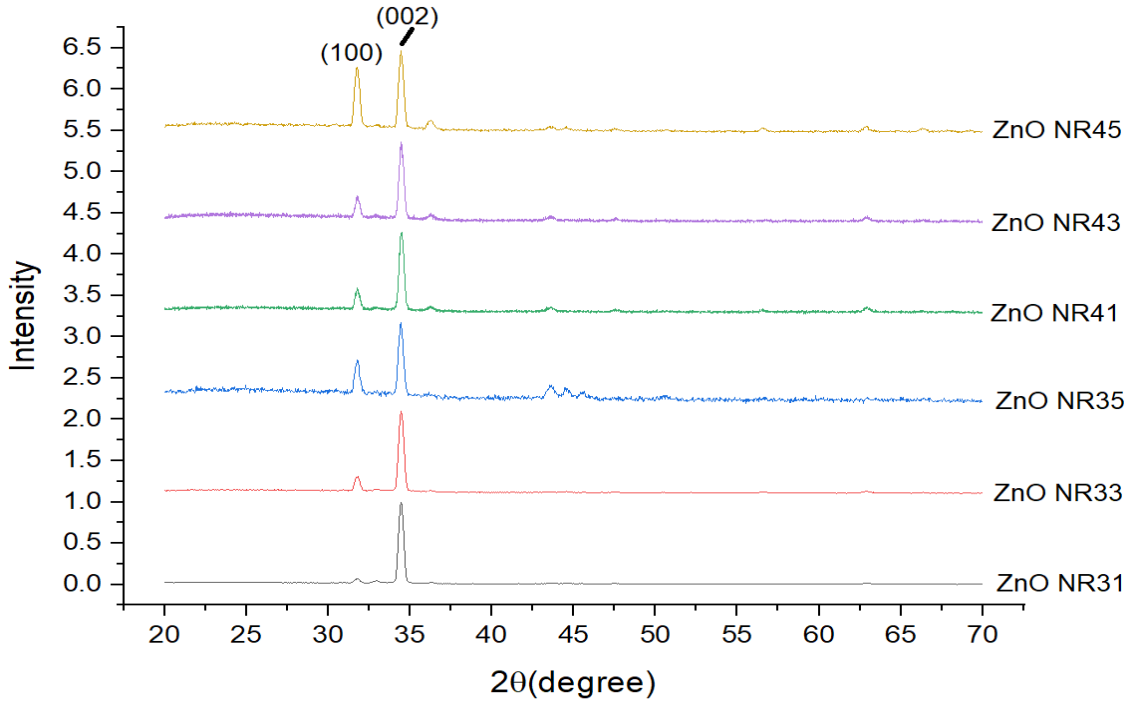

Figure 5 XRD charts of the ZnO NRs, with *v* = 3000 or 4000 rpm, and *n* = 1, 3, or 5

The high intensity of the (002) ZnO peak can be seen in Figure 5, with the 2-theta value around 34.5°. The peak corresponds to the Wurtzite structure of the ZnO NRs. Full width at half maximum (FWHM) analysis was performed on the (002) peak, with origin software used to determine the size of the crystal or grain. The equation used to perform FWHM analysis on the XRD charts in Figure 5 was based on the Scherrer equation, and the parameters are shown in Table 3. By using Scherrer's equation, the crystallite size can be calculated.

Table 3 FWHM analysis of the (002) XRD peak in the ZnO NRs samples

Parameters	NR31	NR33	NR35	NR41	NR43	NR45
Peak Position (°)	34.46	34.47	34.44	34.48	34.48	34.46
FWHM (°)	0.36	0.37	0.38	0.35	0.35	0.36
Crystallite Size (nm)	24.44	23.54	23.20	25.14	24.82	23.91

The values from Table 2 can be put into a chart, as seen in Figure 6. The crystallite size decreases when the number of *n* increases. Such an outcome is the result of the increasing thickness of the seed layer, which provides zinc nuclei to supply larger sized ZnO NRs grains. While this situation gave increased growth along the horizontal direction, as seen in the increased (100) XRD peak, some crystallites from the (002) XRD peak experienced a reduction in size. Such a situation is expected, as growth in crystallite size occurs alongside an increase in film thickness. Meanwhile, higher *v* resulted in less thickness of the seed layer, which reduced the size of the resulting ZnO NRs grains.

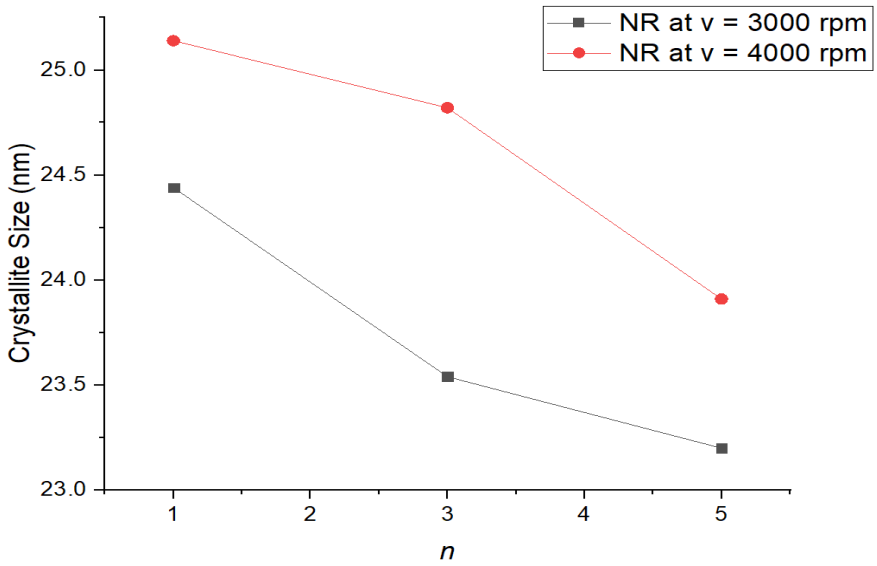

Figure 6 Chart showing the crystallite size of the XRD (002) peak as a function of *n*, shown at *v* = 3000 and 4000 rpm

The Raman spectrum of the ZnO NRs samples is shown in Figure 7. The two most dominant peaks are at E_2(High) and E_2(Low) modes, according to their high and low frequencies of phonons (Manjon et al., 2005). The E_2(Low) peak is related to the vibration of heavy Zn sublattice, while the E_2(High) peak is related to the vibration of oxygen atoms only (Ashkenov et al., 2003). The E_2(High) mode represents the Wurtzite structure of the ZnO NRs. Table 4 shows the FWHM analysis of the E_2(High) peak. This analysis was performed with Spectra Manager software, while the Raman spectrum was obtained from an NRS7100 Raman Spectrometer. It has been found that there is a weakening Wurtzite structure in the ZnO in the case of higher FWHM of E_2(High) (Mu et al., 2016). Therefore, the decrease of FWHM in the Raman E_2(High) peak means that the Wurtzite structure of the ZnO NRs is not distorted. Another point to consider is that the parameters *v* and *n* have not resulted in the shifting of the Raman peaks, which means that the chemical bonds or symmetry are not affected by the parameters *v* and *n*. An unusual chart can be seen in Figure 8, where the value of FWHM as a function of *n* is shown. In the case of *v* = 3000 rpm, the FWHM value decreased when *n* increased. However, in *v* = 4000 rpm, the FWHM decreased at *n* = 3 and increased at *n* = 5. Such a result can be caused by higher *v*, which leads to stronger centrifugal force applied to the sample. When *n* = 3, the resulting seed layer had an increased thickness compared to *n* = 1.

However, when *n* increased to 5, the stronger centrifugal force might damage some structures of the seed layer, which will also distort the Wurtzite structure of the resulting ZnO NRs in the NR45 case.

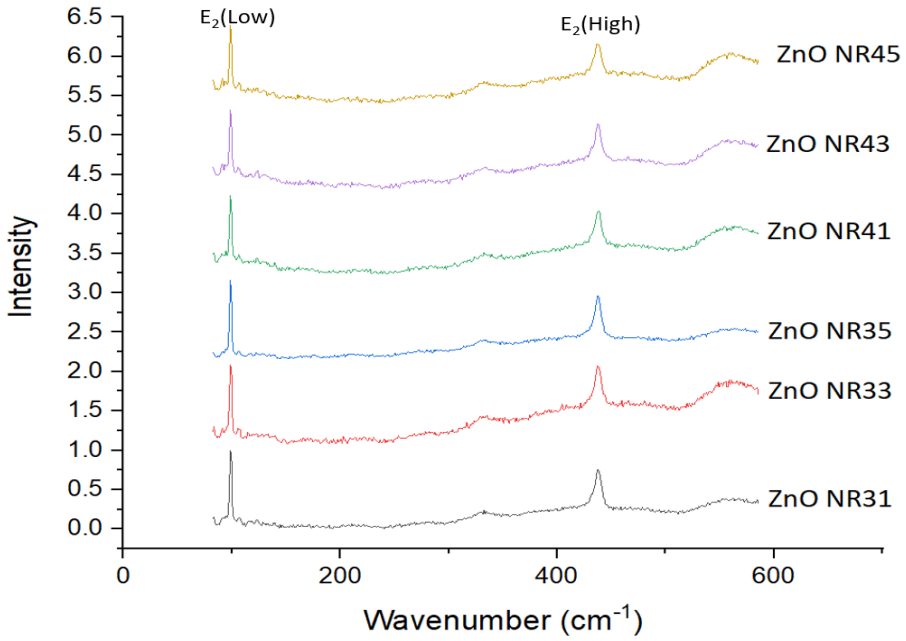

Figure 7 Raman Spectrum of the ZnO NRs; *v* = 3000 or 4000 rpm, and *n* = 1, 3, or 5

Table 4 FWHM analysis of the E_2(High) Raman peak in the ZnO NRs samples

Parameters	NR31	NR33	NR35	NR41	NR43	NR45
Peak Position (cm^{-1})	437.67	437.67	437.67	438.67	437.67	437.67
FWHM (cm^{-1})	7.21	7.07	6.63	7.00	6.00	7.21

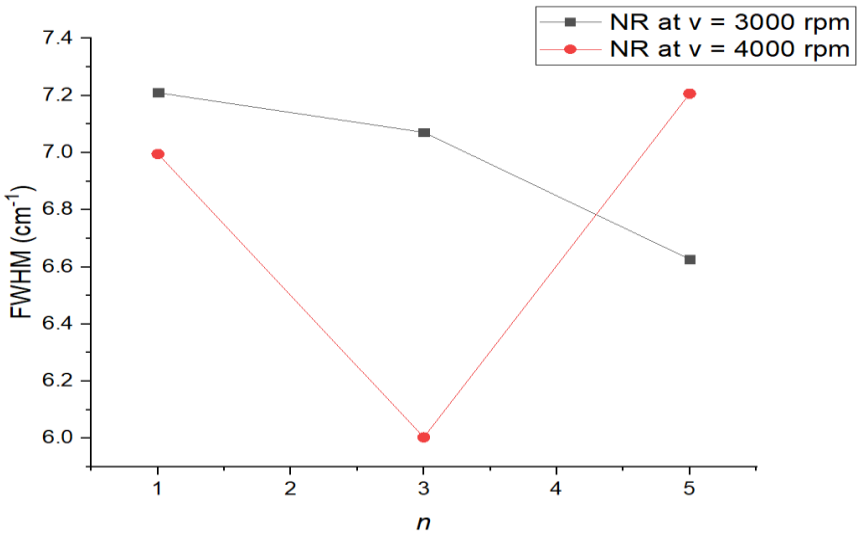

Figure 8 Chart showing the FWHM of the Raman E_2(High) peak as a function of *n*, shown at *v* = 3000 and 4000 rpm

4. CONCLUSION

The effects of the number of the spin coating cycles (*n*) and the rotation speed (*v*) have been discussed in relation to the properties of the ZnO seed layer and the growth of NRs. When the seed layer was spin coated at a higher speed (*v* = 4000 rpm), it tended to become more homogenized, while the preferred orientation deteriorated along the [002] direction. Similar deterioration was also observed in the case of *v* = 3000 rpm. It is believed that a high seed layer density leads to ZnO NRs with high density and fewer empty spaces between each ZnO NR. Under such a condition, the resulting ZnO NRs became less tilted and the XRD results showed stronger [002] ZnO crystallinity. The FWHM of the [002] XRD peak corresponded to the grain or crystal size of the ZnO NRs growing in the c-axis vertical direction. The lowest FWHM of the [002] XRD was obtained by NR31 (*v* = 4000 rpm) at 0.36° and NR41 (*v* = 4000 rpm) at 0.35°. The calculated crystallite sizes from Scherrer's equation yielded 24.44 nm and 25.14 nm consecutively. The crystallite sizes from all the *v* and *n* parameters did not show a wide range of size variation, which showed that the crystallinity of the ZnO NRs was relatively defined for all cases of *v* or *n*. Higher *n* yielded a higher FWHM of the [002] peak, while higher *v* resulted in lower FWHM. The Raman spectrum showed two peaks, corresponding to E_2(High) and E_2(Low) modes. FWHM analysis of E_2(High) corresponded to the Wurtzite structure of the ZnO NRs, and the lowest FWHM of E_2(High) Raman was preferred due to the lower probability of distorted Wurtzite structure. The lowest FWHM of the E_2(High) Raman peak at *v* = 3000 rpm was produced by NR35 at 6.63, while for *v* = 4000 rpm, the lowest FWHM was produced by NR43 at 6.00. For *v* = 3000 rpm, higher *n* yielded a lower FWHM of E_2(High) Raman, while for *v* = 4000 rpm, the FWHM increased at NR45, possibly due to a larger number of oxygen atoms during the ZnO NR growth.

5. REFERENCES

Ashkenov, N., Mbenkum, B.N., Bundesmann, C., Riede, V., Lorenz, M., Spemann, D., Kaidashev, E.M., Kasic, A., Schubert, M., Grundmann, M., Wagner, G., Meumann, H., Darakchieva, V., Arwin, H., Monemar, B., 2003. Infrared Dielectric Functions and Phonon Modes of High-quality ZnO Films. *Journal of Applied Physics*, Volume 93(1), pp. 126–133

Dou, Y., Wu, F., Mao, C., Fang, L., Guo, S., Zhou, M., 2015. Enhanced Photovoltaic Performance of ZnO Nanorod-based Dye-Sensitized Solar Cells by using Ga Doped ZnO Seed Layer. *Journal of Alloys and Compounds*, Volume 633, pp. 408–414

Gautam, K., Singh, I., Bhatnagar, P.K., Peta, K.R., 2016. The Effect of Growth Temperature of Seed Layer on the Structural and Optical Properties of ZnO Nanorods. *Superlattices and Microstructures*, Volume 93, pp. 101–108

Ghayour, H., Rezaie, H.R., Mirdamadi, S., Nourbakhsh, A.A., 2011. The Effect of Seed Layer Thickness on Alignment and Morphology of ZnO Nanorods. *Vacuum*, Volume 86, pp. 101–105

Huang, Q., Fang, L., Chen, X., Saleem, M., 2011. Effect of Polyethyleneimine on the Growth of ZnO Nanorod Arrays and Their Application in Dye-sensitized Solar Cells. *Journal of Alloys and Compounds*, Volume 509(39), pp. 9456–9459

İkizler, B., Peker, S.M., 2014. Effect of the Seed Layer Thickness on the Stability of ZnO Nanorod Arrays. *Thin Solid Films*, Volume 558, pp. 149–159

Kashif, M., Hashim, U., Ali, M.E., Usman Ali, S.M., Rusop, M., Ibupoto, Z.H., Willander, M., 2012. Effect of Different Seed Solutions on the Morphology and Electrooptical Properties of ZnO Nanorods. *Journal of Nanomaterials*, Volume 2012, pp. 106–111

Kim, K.H, Utashiro, K., Abe, Y., Kawamura, M., 2014a. Growth of Zinc Oxide Nanorods using Various Seed Layer Annealing Temperatures and Substrate Materials. *Int. J. Electrochem.*

Sci, Volume 9, pp. 2080–2089

Kim, K.H., Utashiro, K., Abe, Y., Kawamura, M., 2014b. Structural Properties of Zinc Oxide Nanorods Grown on Al-doped Zinc Oxide Seed Layer and Their Applications in Dye-sensitized Solar Cells. *Materials*, Volume 7(4), pp. 2522–2533

Kurda, A.H., Hassan, Y.M., Ahmed, N.M., 2015. Controlling Diameter, Length and Characterization of ZnO Nanorods by Simple Hydrothermal Method for Solar Cells. *World Journal of Nano Science and Engineering*, Volume 5, pp. 34–40

Manjon, F.J., Mari, B., Serrano, J., Romero, A.H., 2005. Silent Raman Modes in Zinc Oxide and Related Nitrides. *Journal of Applied Physics*, Volume 97(5), pp. 053516-1– 053516-4

Mu, J., Guo, Z., Che, H., Zhang, X., Bai, Y., Hou, J., 2016. Electrospinning of C-doped ZnO Nanofibers with High Visible-light Photocatalytic Activity. *Journal of Sol-Gel Science and Technology*, Volume 78(1), pp. 99–109

Peiris, T.A.N., Alessa H., Sagu, J.S., Bhatti, I.A., Isherwood, P., Wijayantha, K.G.U., 2013. Effect of Zno Seed Layer Thickness on Hierarchical Zno Nanorod Growth on Flexible Substrates for Application in Dye-sensitised Solar Cells. *Journal of Nanoparticle Research*, Volume 15, pp. 1–10

Poornajar, M., Marashi, P., Fatmehsari, D.H., Esfahani, M.K., 2016. Synthesis of Zno Nanorods via Chemical Bath Deposition Method: The Effects of Physicochemical Factors. *Ceramics International*, Volume 42(1), pp. 173–184

Pourshaban, E., Abdizadeh, H., Golobostanfard, M.R., 2015. ZnO Nanorods Array Synthesized by Chemical Bath Deposition: Effect of Seed Layer Sol Concentration. *Procedia Materials Science*, Volume 11, pp. 352–358

Sholehah, A., Yuwono, A.H., 2015. The Effects of Annealing Temperature and Seed Layer on the Growth of ZnO Nanorods in a Chemical Bath Deposition Process. *International Journal of Technology*, Volume 6(4), pp. 565–572

Sholehah, A., Yuwono, A.H., Sofyan, N., Hudaya, C., Amal, M.I., 2017. Effect of Post- hydrothermal Treatments on the Physical Properties of ZnO Layer Derived from Chemical Bath Deposition. *International Journal of Technology*, Volume 8(4), pp. 651–661

Song, J., Lim, S., 2007. Effect of Seed Layer on the Growth of ZnO Nanorods. *The Journal of Physical Chemistry C*, Volume 111(2), pp. 596–600

Wahid, K.A., Lee, W.Y., Lee, H.W., Teh, A.S., Bien, D.C., Azid, I.A., 2013. Effect of Seed Annealing Temperature and Growth Duration on Hydrothermal Zno Nanorod Structures and Their Electrical Characteristics. *Applied Surface Science*, Volume 283, pp. 629–635

Winantyo, R., Murakami, K., Nusantara, R.W.U.M., 2017. ZnO Nanorods Formation for Dye-sensitized Solar Cells Applications. *International Journal of Technology*, Volume 8(8), pp. 1462–1469

Yoon, Y,C., Park, K.S., Kim, S.D., 2015. Effects of Low Preheating Temperature for Zno Seed Layer Deposited by Sol–gel Spin Coating on the Structural Properties of Hydrothermal Zno Nanorods. *Thin Solid Films*, Volume 597, pp. 125–130